

# A mathematical model of *B. thetaiotaomicron*, *M. smithii*, and *E. rectale* interactions in the human gut

Melissa A. Adrian<sup>1+\*</sup>, Bruce P. Ayati<sup>1</sup>, and Ashutosh K. Mangalam<sup>2</sup>

<sup>1</sup>University of Iowa, Department of Mathematics, Iowa City, IA, 52242, USA

<sup>2</sup>University of Iowa, Department of Pathology, Iowa City, IA, 52242, USA

\*maadrian@uchicago.edu

<sup>+</sup>Current Affiliation: University of Chicago, Department of Statistics, Chicago, IL 60637

## ABSTRACT

The human gut microbiota is a complex ecosystem that affects a range of human physiology. In order to explore the dynamics of the human gut microbiota, we used a system of ordinary differential equations to mathematically model the biomass of three microorganism populations: *Bacteroides thetaiotaomicron*, *Eubacterium rectale*, and *Methanobrevibacter smithii*. Additionally, we modeled the concentrations of relevant nutrients necessary to sustain these populations over time. Our model highlights the interactions and the competition among these three species. These three microorganisms were specifically chosen due to the system's end product, butyrate, which is a short chain fatty acid that aids in developing and maintaining the intestinal barrier in the human gut. The basis of our mathematical model assumes the gut is structured somewhat similar to a chemostat, with bacteria and nutrients exiting the gut at a rate proportional to the volume of the chemostat, the rate of volumetric flow, and the biomass or concentration of the particular population or nutrient. We performed global sensitivity analyses using Sobol' sensitivities to estimate the relative importance of model parameters on simulation results.

## Introduction

The human gut microbiota is the collection of microorganisms located in the stomach, large intestines, and small intestines, and this system plays an important role in sustaining overall human health. Each individual's gut composition is unique, and, besides the host's genetic makeup, their long-term dietary patterns, specifically concerning the types and amounts of carbohydrates, proteins, and fats consumed, affect its composition<sup>1,2</sup>. Specifically, gut microbiota have been shown to be involved in numerous physiological processes, such as digestion of undigested food (complex starch), development and regulation of immune system, blocking growth of pathogens, and generation of neurotransmitter and vitamins. Thus, any changes in environmental conditions in this gut ecosystem (microbiota) can result in a shift in its composition, which can predispose and/or worsen chronic inflammatory diseases such as inflammatory bowel diseases, multiple sclerosis, rheumatoid arthritis and neurological diseases like Alzheimer's disease, Parkinson disease and autism<sup>3-5</sup>. Though the changes in the bacterial composition of the human gut microbiota have been shown to be associated with rapid changes in metabolism and overall health, the underlying interactions among species within this microbiota are not yet well understood<sup>2</sup>. Among all the factors linked with regulation of gut microbiota, diet has emerged as the strongest as it can override genetic influences on microbiota<sup>6,7</sup>. A better understanding of the microbial dynamics, particularly mathematical approaches, may elucidate the role that the gut microbiota plays in human diseases<sup>1</sup>.

Common approaches to analyzing the human gut microbiota for its diversity and composition include, but are not limited to, next-generation sequencing, metatranscriptomics, culturomics, and mass spectrometry analyses<sup>2,8</sup>. These approaches give little insight as to how species interact amongst themselves and with the human host<sup>2</sup>. Mathematical modeling, however, attempts to answer such questions and can supplement the knowledge gained from these common approaches. Mathematical models can provide evidence to strengthen a hypothesis about these interactions and offer guiding principles for further study of a phenomenon<sup>9</sup>.

We use ordinary differential equation (ODE)-based modeling as the main tool for our analysis, which tracks information about biomass and concentration levels over time rather than genomic information as in the case of GEMs. In this so-called dynamical system approach, we can identify the system's driving parameters and analyze its stability. Despite the advantage of having easily interpretable terms in the model's equations, this approach still has some key drawbacks, specifically the determination of unknown parameters.

The parameters used in biological models like ours include substrate conversion rates, utilization rates, and cellular death rates, which typically can be determined and validated by laboratory experiments. However, some gut microorganisms are unable to be cultivated in a laboratory setting, leaving specific information about these species' metabolic activity unknown.

Additionally, ODE models are often used to track only a small subset of species within a community. While this is often due to the difficulty of determining a larger number of parameters when the system is expanded<sup>8</sup>, focusing on a few subspecies at a time may aid in identifying the dominant relationships in that subsystem.

Despite the impracticality of ODE-based modeling for some very large systems, ODE models paired with other types of modeling, such as agent-based modeling, can provide an insightful understanding of the gut microbiota's dynamics and interactions<sup>8</sup>. As a first step in our modeling efforts with its limitations in mind, we consider an ODE-based modeling approach for a small-scale system of three abundant microorganisms in the human gut microbiota. Our ODE model is structured similar to models of chemostats, which are idealized laboratory systems for microbial ecology that have a long history of mathematical modeling behind it<sup>10</sup>. One contribution of this paper is the use of a similar approach, rather than the "batch" models in other gut microbiome models<sup>8</sup>, so that the vital role of the inflows and outflows in the human gut ecosystem has a more faithful representation.

We focus our representation on a subsystem of the human gut microbiota. The three microorganisms *Bacteroides thetaiotaomicron*, *Eubacterium rectale*, and *Methanobrevibacter smithii* were chosen to be the focus of our model. These species represent the three main phyla in the human gut: Bacteroidetes, accounting for 17-60% of the total biomass; Firmicutes, 35-80% of the biomass; and Euryarchaeota the bulk of the remainder<sup>11</sup>. The system's main product, butyrate, is of specific interest due to its role in sustaining human health. Butyrate provides energy to colonocytes, affects overall energy homeostasis, and inhibits histone deacetylase, which is an enzyme that directly affects colorectal cancer<sup>11</sup>. Along with butyrate, other notable intermediates and products in this system include acetate, propionate, glutamine, carbon dioxide (CO<sub>2</sub>), hydrogen (H<sub>2</sub>), and methane (CH<sub>4</sub>). Acetate, propionate, and butyrate, which are short chain fatty acids, are absorbed in the gut's epithelial cells and regulate an individual's immune system and metabolism<sup>11</sup>. Individually, acetate acts as a substrate for cholesterol synthesis and lipogenesis<sup>11</sup>; propionate regulates gluconeogenesis and cholesterol synthesis<sup>11</sup>; glutamine fuels the metabolism and maintains the intestinal barrier<sup>12</sup>; and the gases CO<sub>2</sub>, H<sub>2</sub>, and CH<sub>4</sub> are products of bacterial fermentation that can cause intestinal discomfort in excess<sup>13</sup>. As for the microorganisms themselves, *M. smithii* removes hydrogen gas, which affects bacterial fermentation and energy gathering, and produces methane gas<sup>11</sup>; *E. rectale* produces butyrate, which is beneficial to the gut's epithelial cells<sup>11</sup>; and *B. thetaiotaomicron* utilizes dietary polysaccharides and indirectly facilitates butyrate production with its outputs<sup>2</sup>.

In our model, we represent the interactions of three short chain fatty acid producing/utilizing gut microorganisms (see Figure 1) and their metabolites. *B. thetaiotaomicron* is an abundant bacterial species in the human gut microbiome whose main function is the utilization of polysaccharides<sup>2,14</sup>. Through polysaccharide degradation, *B. thetaiotaomicron* contributes to the overall ecosystem diversity in the colon, which is its regular environment<sup>15</sup>. *B. thetaiotaomicron* can survive solely on the uptake of carbon-rich polysaccharides<sup>16</sup>; however, its growth is enhanced in the presence of inorganic ammonia due to inorganic ammonia's contribution of nitrogen to *B. thetaiotaomicron*'s metabolism<sup>17</sup>. Through the utilization of inorganic ammonia, *B. thetaiotaomicron* can synthesize all amino acids that are essential to human health<sup>2</sup>, which makes this bacteria a focus of study.

When both *E. rectale* and *B. thetaiotaomicron* are present in an environment, *B. thetaiotaomicron* up-regulates gene expression for starch utilization and the degradation of specific glycans that *E. rectale* is unable to utilize. Simultaneously, *E. rectale* down-regulates the genes associated with glycan degradation even though it cannot grow efficiently without a carbohydrate source. Previous research on the interactions of these two species suggests that the presence of *B. thetaiotaomicron* enhances *E. rectale*'s ability to uptake nutrients<sup>18</sup>. *E. rectale* shifts from uptaking polysaccharides to utilizing amino acids, such as glutamine, when *B. thetaiotaomicron* is present<sup>2</sup>.

*M. smithii*, which is one of the main methanogenic archaeon in the human gut, improves the productivity of carbohydrate metabolism by utilizing H<sub>2</sub> from *E. rectale* and formate from *B. thetaiotaomicron* to produce methane gas. This process prevents the environment from becoming too saturated with *B. thetaiotaomicron* and *E. rectale*'s by-products, which consequently improves carbohydrate metabolism. Additionally, *M. smithii* removing H<sub>2</sub> in this environment allows for *B. thetaiotaomicron* to generate NAD<sup>+</sup>, which is used for glycolysis, a fundamental process in producing cellular energy<sup>18</sup>.

The information known about these three species' interactions is translated into a graphical representation in Figure 1. This schematic highlights the competition among these species, specifically between *E. rectale* and *M. smithii* and between *B. thetaiotaomicron* and *E. rectale*.

The results of our modeling effort suggest the efficacy of a relatively simple ODE approach, similar to those used for chemostats, in understanding and potentially predicting the dynamics of important subsystems in the larger human gut ecosystem.

## Results

Using our mathematical model of *Bacteroides thetaiotaomicron*, *Eubacterium rectale*, and *Methanobrevibacter smithii* and their metabolites in equations 1 and 2, we present numerical results, estimation of key parameters, and sensitivity analysis.

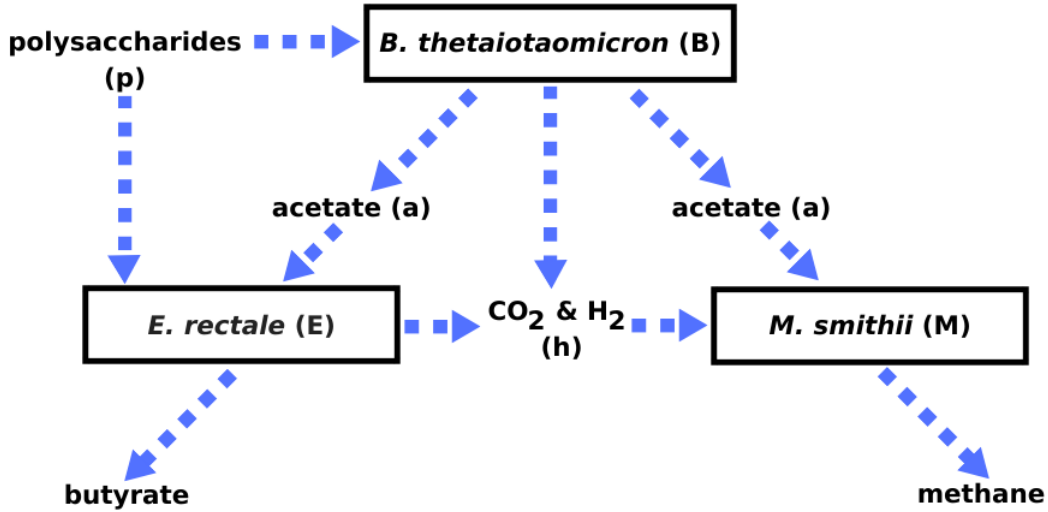


**Figure 1.** Graphical representation of the interactions of the three species, *B. thetaiotaomicron*, *E. rectale*, and *M. smithii*, and their metabolites. Each microorganism or substance given a letter is included in the mathematical model equations. This figure was developed from information presented in Ji & Nielsen 2015<sup>2</sup>, Shoaie et al. 2013<sup>11</sup>, and Adamberg et al. 2014<sup>15</sup>.

## Numerical Results

Using the set of parameter estimates in Table 5, the solutions to our full model are given for the dynamics of *B. thetaiotaomicron*, *M. smithii*, and *E. rectale* in Figure 2, for acetate in Figure 3, for CO<sub>2</sub> and H<sub>2</sub> in Figure 4, and for polysaccharides in Figure 5. These plots show the solutions to our full system of ODEs in equations (1) and (2) from 1,000 to 1,100 hours. This time range was selected in order to allow for a sufficient amount of time to pass in order for the system to converge to a regular oscillation. The center values of the oscillations are represented by dotted lines in each plot. In Figures 3, 4, and 5, the data values given in Table 3 are superimposed on their respective plots as dashed lines in order to provide a visual representation of the error between the mean of the regular oscillation and the observed data. Despite some error in the center value of the ODE solutions compared to the data, the observed data values for acetate, polysaccharides, and the gases CO<sub>2</sub> and H<sub>2</sub> are contained in the oscillation range of the ODEs' numerical solutions, so we conclude that our parameter estimates sufficiently fit the data. Thus, the relatively simple model we have presented here is consistent with the data in our literature review.

## Sensitivity Analysis

Based on the fitted parameter values and the available data from the literature, we analyzed our model's sensitivity to its parameters. In order to identify the parameters in the model that have the greatest effect on the model output, we conducted sensitivity analysis on our model by computing the first- and total-order effects based on Sobol' indices.

Sensitivity analysis can be defined as the study of how uncertainty in the model input propagates into uncertainty in the model output<sup>19</sup>. Once parameters are estimated, sensitivity analysis can be used to identify the driving parameters of the system that contribute to the most variability in the model's output. Sensitivity analysis tests the robustness of the model, identifies if the model relies on weak assumptions, and allows for model simplification<sup>19</sup>.

The results of our sensitivity analysis using the methods described in the section titled "Sensitivity Analysis Methods" are given in Tables 6 and 7.

Using our code in Appendix A to produce the first- and total-order Sobol' indices for our full ODE model, we obtained the results seen in Tables 6 and 7. Based on Table 6 of the first-order Sobol' indices,  $\beta_B$  is an influential parameter for *B. thetaiotaomicron*'s output variance;  $\beta_{E_2}$  for *E. rectale*'s variance;  $\beta_{M_2}$  for *M. smithii*'s variance; no first-order parameter for acetate's variance;  $\beta_B$  and  $\beta_{M_2}$  for CO<sub>2</sub> and H<sub>2</sub>'s variance; and  $\beta_B$  for polysaccharides' variance. Based on Table 7 of the total-order Sobol' indices,  $\beta_B$  is an influential parameter for *B. thetaiotaomicron*'s output variance;  $\beta_{E_2}$  and  $\beta_B$  for *E. rectale*'s variance;  $\beta_{M_2}$ ,  $q$ , and  $\beta_B$  for *M. smithii*'s variance;  $\beta_B$ ,  $\beta_{E_1}$ ,  $\beta_{E_2}$ ,  $\beta_{M_1}$ ,  $\beta_{M_2}$ , and  $q$  for acetate's variance;  $\beta_B$ ,  $\beta_{E_2}$ ,  $\beta_{M_1}$ ,  $\beta_{M_2}$ , and  $q$  for CO<sub>2</sub> and H<sub>2</sub>'s variance; and  $\beta_B$ ,  $\beta_{E_2}$ , and  $q$  for polysaccharides' variance. Based on the changes in the estimated indices from first-order to total-order indices, there appears to be a higher-order interaction among model parameters for *E. rectale*'s, *M. smithii*'s, acetate's, CO<sub>2</sub> and H<sub>2</sub>'s, and polysaccharides' output variance. We note that observing Sobol' indices whose sum is greater than 1, as seen in Table 7, is evidence of potentially correlated inputs in the model<sup>20</sup>. Overall, the two main driving parameters of the ODE model appear to be the reproduction coefficient for *B. thetaiotaomicron* ( $\beta_B$ ) and the ratio of the volume

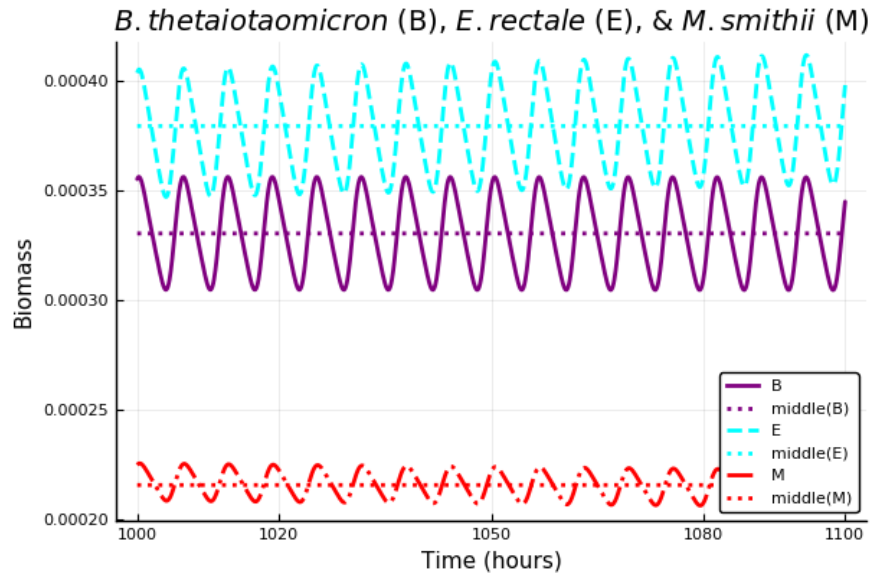


**Figure 2.** Plot of the solutions to equations (1a), (1b), and (1c) using the observed data in Table 3 over the time interval 1,000 to 1,100 hours. Based on Table 3, the sum of the three species' biomass should be 0.001412 gDW. The middle of the solutions to the ODEs using the parameter estimates in Table 5 for all three species sums to 0.000925 gDW, resulting in an error of  $-0.000487$  gDW.

of the chemostat over the volumetric flow ( $q$ ). Because these parameters are identified to be sensitive to perturbations, careful attention needs to be given to estimating these parameters and reducing the error of their estimates in future efforts.

## Discussion

We suggest and illustrate that a mathematical representation similar to those for chemostats is a natural way to capture the effects of the inflow and outflow in the gut on its microbial dynamics.

The three species chosen to be the focus of our model, *B. thetaiotaomicron*, *E. rectale*, and *M. smithii*, play an important role in polysaccharide degradation and the production of butyrate, which both aid in the human gut's ability to absorb nutrients through the epithelial cells<sup>11</sup>. The system of the three microbial species has been considered in previous works<sup>2,11</sup>, which largely informed our knowledge of this system. By creating a mathematical model based on the interactions of these species, we have analyzed their interactions and identified aspects of this system that should be further explored through empirical investigation.

Due to the limited availability of data for a more rigorous parameter estimation, our sensitivity analysis took on additional importance. Through the results of the sensitivity analysis using first- and total-order Sobol' indices, we more narrowly identified specific links in the microbial food web that would be fruitful targets for additional empirical work. Specifically, we identified the growth rate coefficients  $\beta_B$ ,  $\beta_{E_1}$ ,  $\beta_{E_2}$ ,  $\beta_{M_1}$ ,  $\beta_{M_2}$ , and the scaled volumetric flow ( $q$ ) as being largely significant in contributing to the variance of the model output, including higher-order interactions among these parameters. With these results, we suggest that estimates of these significant parameters be obtained through laboratory experimentation in order to capture these values to a higher degree of precision and accuracy.

The significant growth rate coefficients ( $\beta$  parameters) correspond to the growth rates of the three microorganisms when supported on a medium containing specific nutrients. Experiments should focus on cultivating these microorganisms in isolation in germ-free mice with only one nutrient<sup>11</sup>. Despite the fact that these microorganisms are able to be cultured in isolation of other microorganisms, they may not be able to be sustained on one single nutrient, but rather require the presence of additional substrates. In this case, nonlinear effects from these secondary nutrients would factor in to the resulting estimates of the growth parameters. Table 2 provides a general outline of the specific nutrient and microorganism necessary to estimate each parameter. For example, the growth rate coefficient for *B. thetaiotaomicron* ( $\beta_B$ ) can be experimentally estimated by cultivating *B. thetaiotaomicron* in a medium containing only polysaccharides. Additionally, experiments approximating the rate of flow of the digestive system's fluids would largely inform the estimate for the true value of the volumetric flow rate parameter  $q$ .

Due to the possibility of correlation among model parameters, variance-based sensitivity analyses specifically for correlated parameters should be explored and applied to this system, such as the methods discussed in Iooss and Prieur 2019<sup>20</sup> and Rabitz

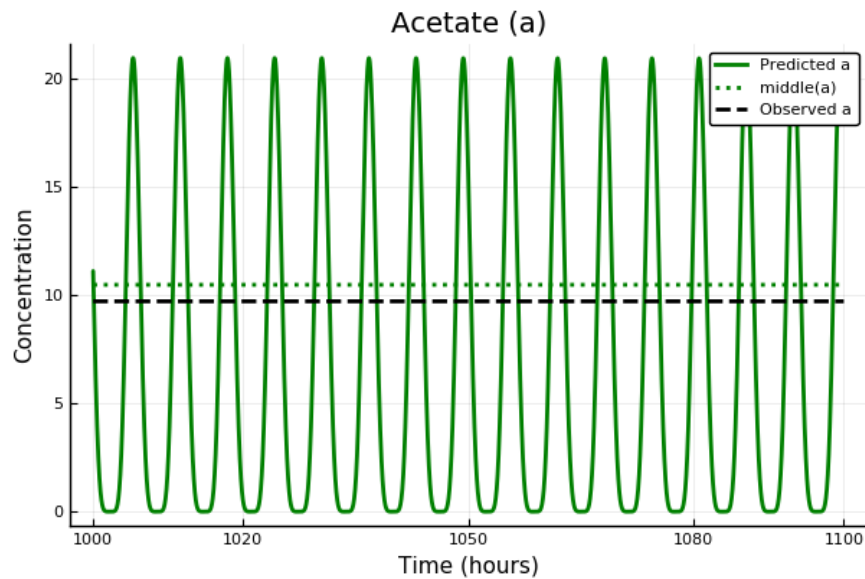


**Figure 3.** Plot of the solutions to equation (2a) using the observed data in Table 3 over the time interval 1,000 to 1,100 hours. Based on Table 3, the center of acetate’s oscillations should be  $9.71 \mu\text{M}$ . The middle concentration of the ODE solutions for acetate is  $10.47 \mu\text{M}$ , resulting in a  $0.76 \mu\text{M}$  error.

2010<sup>21</sup>. In regards to specifying the prior distributions on parameters, further analyses should include testing differing prior parameter distributions in order to compute the Sobol’ indices, especially to explore the amount of variability in results based on the chosen parameter distributions<sup>19</sup>.

Our main suggestion for future work is to collect more complete longitudinal data on this biological system, including for all three species *B. thetaiotaomicron*, *E. rectale*, and *M. smithii* and its relevant substrates. With this experimental data, more precise estimates of the model parameters can be achieved. With this approach, particular attention can be paid to estimating the parameters that were identified as sensitive by the Sobol’ indices.

Additionally, further extensions of our model may include relaxing some of the assumptions of a general chemostat model. Specifically, the rate of volumetric flow through the chemostat can be generalized to reflect aspects of the natural flow of the gut, such as periodically restricted flow, and the framework of a single vessel representation can be extended to consider additional compartments to mimic the system of digestive organs in the human body. Aside from the assumptions of a simple chemostat model, future implementations of a similar model can account for absorption rate of substrates within the gut, which is especially important to consider for substances like amino acids. With these potential improvements of our baseline model, additional aspects about the dynamics of this biological system can be uncovered, and these improvements to our model could fuel further research directions related to this system.

Our model has relevance to human microbiome studies as it can be used to test the significance of clinical findings. For example, microbiome studies for human autoimmune disease, such as multiple sclerosis, have shown modulation of butyrate and methane-producing gut bacteria<sup>22</sup>. This can be incorporated into our modeling framework in combination with experimental studies to determine the mechanism through which gut bacterial modulate disease.

## Methods

The key assumption underlying our mathematical model is that the human gut can be represented as a chemostat. A chemostat is a laboratory device used in the simulation and ecological study of populations, which provides an idealized representation of naturally occurring phenomena and has a rich history of mathematical representation. Though the conditions of a chemostat are simplified and controlled in a laboratory setting, a chemostat can be useful in the study of population dynamics and the underlying mechanisms of interactions among populations. The simple chemostat model is a first step in developing an initial theoretical framework, which can then be refined and extended<sup>10</sup>.

In developing an ODE model to represent our chosen microbiota subsystem, we assume that the human gut acts in a manner similar to that of a chemostat, which is an approach not used, to our knowledge, in other work. We utilize ODE-based dynamical systems modeling to track the changes in biomass of the three prevalent microorganisms, *B. thetaiotaomicron*, *E. rectale*, and *M. smithii*, as well as their chemical inputs, intermediates, and byproducts, with the goal of providing a better

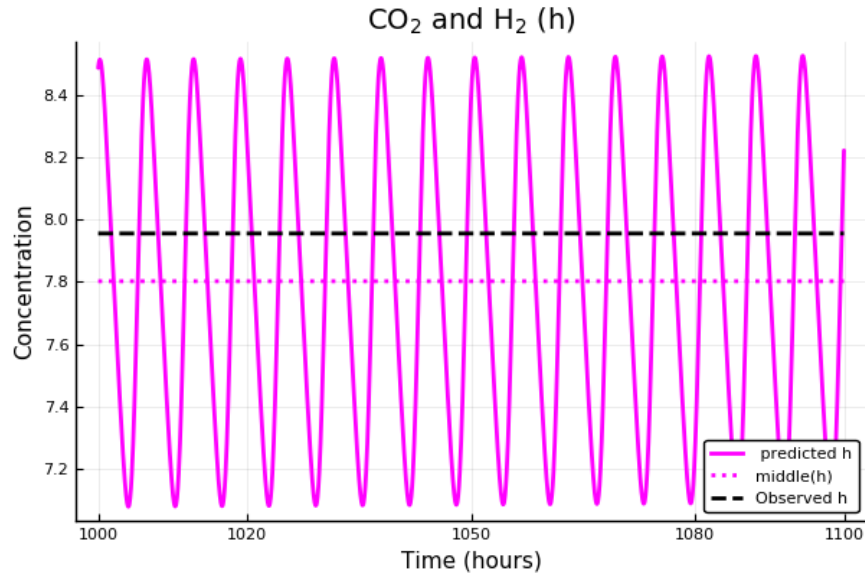


**Figure 4.** Plot of the solutions to equation (2b) using the observed data in Table 3 over the time interval 1,000 to 1,100 hours. Based on Table 3, the center of CO<sub>2</sub> and H<sub>2</sub>'s oscillations should be roughly 7.96 μM. The middle concentration of the ODE solutions for CO<sub>2</sub> and H<sub>2</sub> is 7.80 μM, resulting in a −0.16 μM error.

understanding of their interactions within this subsystem.

In order to supplement the knowledge gained from transcriptomic analysis and GEMs, we incorporate this information into our own mathematical interpretation of this small-scale system using ODEs. Throughout our model explanation, we present information learned through previous investigations of *B. thetaiotaomicron*, *E. rectale*, and *M. smithii* that we utilized in creating our mathematical model.

In constructing a first chemostat model, we assume that the contents of the vessel are well-mixed, the rate at which liquid enters the system equals the rate at which the well-stirred contents leave the compartment, and that some significant factors potentially affecting growth, such as temperature, are held constant<sup>10</sup>.

For specificity we assume that microorganisms grow at a rate following the Monod form

$$\beta_X \left( \frac{u}{u + \gamma} \right) X,$$

where  $\beta_X$  is the maximum birth rate of population  $X$ ,  $u$  is the concentration of the nutrient population on which  $X$ 's growth depends,  $\gamma$  is the Michaelis-Menten constant, and  $X$  is the concentration of the microorganism<sup>23</sup>. This form is commonly used, especially for a first effort. Other functional forms that could be used include Hill functions<sup>24</sup>, which are generalizations of the Monod form, and S-forms<sup>25</sup>. The accompanying large increase in the number of parameters, and lack of data to capture the detail these parameters provide, means that they are less appropriate for our effort here than the Monod form.

### Model Variables

The variables in our model for the microbial and chemical species depend only on one independent variable, time, denoted by  $t$ . These dependent variables are

- $B$  for *B. thetaiotaomicron*,
- $E$  for *E. rectale*,
- $M$  for *M. smithii*,
- $a$  for acetate,
- $h$  for CO<sub>2</sub> and H<sub>2</sub>,
- $p$  for polysaccharides.

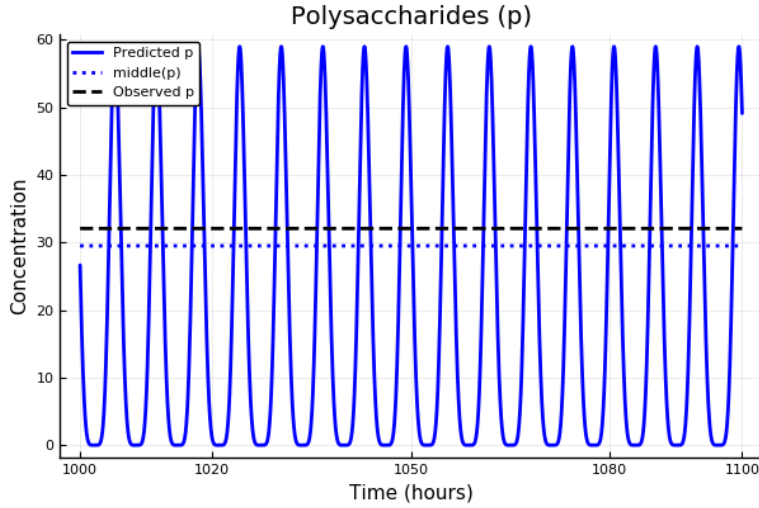


**Figure 5.** Plot of the solutions to equation (2c) using the observed data in Table 3 over the time interval 1,000 to 1,100 hours. Based on Table 3, the center of polysaccharides' oscillations should be roughly  $32.06 \mu\text{M}$ . The middle concentration of the ODE solutions for polysaccharides is  $29.50 \mu\text{M}$ , resulting in a  $-2.56 \mu\text{M}$  error.

### Model Equations

The equations for the three microbial species are

$$\frac{dB}{dt} = \beta_B \Psi_{\gamma_p}(p)B - qB, \quad (1a)$$

$$\frac{dE}{dt} = [\beta_{E_1} \Psi_{\gamma_a}(a) + \beta_{E_2} (1 - \Psi_{\gamma_B}(B)) \Psi_{\gamma_p}(p)] E - qE, \quad (1b)$$

$$\frac{dM}{dt} = [\beta_{M_1} \Psi_{\gamma_a}(a) + \beta_{M_2} \Psi_{\gamma_h}(h)] M - qM. \quad (1c)$$

The equations for the three chemical species are

$$\frac{da}{dt} = \beta_a \Psi_{\gamma_p}(p)B - qa - [\mu_{a,E}E + \mu_{a,M}M]a, \quad (2a)$$

$$\frac{dh}{dt} = \beta_{h_1} \Psi_{\gamma_a}(a)E + \beta_{h_2} \Psi_{\gamma_p}(p)B - qh - \mu_{h,M}hM, \quad (2b)$$

$$\frac{dp}{dt} = \beta_p q (\cos(t) + 1)^3 - qp - [\mu_{p,B}B + \mu_{p,E}E]p. \quad (2c)$$

The  $\Psi$  and  $q$  terms in these equations are defined by

$$\Psi_{\gamma}(u) = \frac{u}{u + \gamma}, \quad (3)$$

$$q = \frac{V}{Q}. \quad (4)$$

In our model we assume that there is a high enough rate of turnover of fluids in the human gut such that these microorganisms are almost always flushed out of the system before their life expectancy, so death terms are neglected in these three equations. All three microorganism equations thus have the general format:

$$\Delta_i = P_{ij} - F_i,$$

where  $\Delta_i$  is the rate of change of biomass for microorganism  $i$ ,  $P_{ij}$  is the rate at which microorganism  $i$  proliferates based on the availability of substance  $j$ , and  $F_i$  is the rate at which microorganism  $i$  is flushed out of the gut. In all three microorganism equations, the term  $F_i$  is the biomass of the given population multiplied by the constant  $q$ . The fixed quantity  $q$  is interpreted as

	$k$	$\theta$	Mean	Variance
$\beta_a$	$5.00 \times 10^6$	2.00	$1.00 \times 10^7$	$2.00 \times 10^7$
$\beta_B$	0.60	2.00	1.20	2.40
$\beta_{E_1}$	0.40	2.00	0.80	1.60
$\beta_{E_2}$	0.30	2.00	0.60	1.20
$\beta_{h_1}$	75.00	2.00	150.00	300.00
$\beta_{h_2}$	$1.67 \times 10^4$	2.00	$3.33 \times 10^4$	$6.67 \times 10^4$
$\beta_{M_1}$	0.40	2.00	0.80	1.60
$\beta_{M_2}$	0.25	2.00	0.50	1.00
$\beta_p$	$5.00 \times 10^3$	2.00	$1.00 \times 10^4$	$2.00 \times 10^4$
$\gamma_a$	100.00	2.00	200.00	400.00
$\gamma_B$	5.00	2.00	10.00	20.00
$\gamma_h$	75.00	2.00	150.00	300.00
$\gamma_p$	200.00	2.00	400.00	800.00
$\mu_{aE}$	$1.25 \times 10^3$	2.00	$2.50 \times 10^4$	$5.00 \times 10^4$
$\mu_{aM}$	$2.50 \times 10^4$	2.00	$5.00 \times 10^4$	$1.00 \times 10^5$
$\mu_{hM}$	20.00	2.00	40.00	80.00
$\mu_{pB}$	$1.00 \times 10^5$	2.00	$2.00 \times 10^5$	$4.00 \times 10^5$
$\mu_{pE}$	$2.50 \times 10^3$	2.00	$5.00 \times 10^3$	$1.00 \times 10^4$
	$\alpha$	$\beta$	Mean	Variance
$q$	5.00	95.00	0.05	$4.70 \times 10^{-2}$

**Table 1.** Table of specified distributions for the parameters in our full model, including the mean and variance of each distribution. The parameters whose distribution is specified with  $k$  and  $\theta$  follow a Gamma( $k, \theta$ ) distribution. The parameter  $q$ , however, follows a Beta( $\alpha, \beta$ ) distribution.

Parameter	Microorganism	Nutrient
$\beta_B$	<i>B. thetaiotaomicron</i>	polysaccharides
$\beta_{E_1}$	<i>E. rectale</i>	acetate
$\beta_{E_2}$	<i>E. rectale</i>	polysaccharides
$\beta_{M_1}$	<i>M. smithii</i>	acetate
$\beta_{M_2}$	<i>M. smithii</i>	CO <sub>2</sub> and H <sub>2</sub>

**Table 2.** Table of microorganism growth rate parameters suggested to be estimated experimentally.

the rate at which the contents of the gut leave the system as expressed in equation (4), where  $V$  is the volume of the chemostat and  $Q$  is the rate of volumetric flow within the chemostat<sup>10</sup>.

In order for *E. rectale* to grow in biomass, acetate or polysaccharides need to be present in the ecosystem<sup>11</sup>. We assume that *E. rectale* has different maximum growth rates depending on each nutrient, leading us to split  $\beta_E$  into three different, related constants. Because *E. rectale* shifts to uptaking inorganic ammonia when *B. thetaiotaomicron* is present, we included the term  $(1 - \Psi_{\gamma_B}(B))$  to reflect this shift. *M. smithii* depends on the presence of acetate and the gases CO<sub>2</sub> and H<sub>2</sub>, which are both incorporated in the standard Monod form. Again, we assume that *M. smithii* grows at different maximum growth rates in the presence of only one of these metabolites, which lead to the separation of  $\beta_M$  into the constants  $\beta_{M_1}$  and  $\beta_{M_2}$ .

The metabolite equations detail the rates of change over time for the intermediate substances produced and consumed by these three species, where the concentrations are tracked for acetate in equation (2a), CO<sub>2</sub> and H<sub>2</sub> in equation (2b), and polysaccharides in equation (2c). These concentrations depend on the rate at which these metabolites are produced by the microorganisms or enter into the system, the rate at which they are flushed out of the system, and the rate at which they are consumed by surrounding microorganisms. All five metabolite equations are constructed in the general format:

$$\Delta_j = P_{ij} - F_j - C_{ij},$$

where  $\Delta_j$  is the rate of change of metabolite  $j$ 's concentration,  $P_{ij}$  is the rate at which metabolite  $j$  is produced by microorganism

$i$  or enters the system,  $F_j$  is the rate at which metabolite  $j$  is flushed out of the chemostat, and  $C_{ij}$  is the rate at which the metabolite  $j$  is consumed by microorganism  $i$ . In each of the metabolite equations, the parameter  $\mu_{x,Y}$  is the rate at which substance  $x$  is utilized by species  $Y$ .

Polysaccharides enter the human gut through diet, so we accounted for their addition to the gut through a sinusoidal function,  $(\cos(t) + 1)^3$ . This function attempts to account for the duration of time in between meals through the period of the curve. In addition, this function is defined to be a smooth curve to illustrate the gradual breakdown of food and release of nutrients in the gut.

### Parameter Estimation Techniques

In our model, many of the parameter values are unknown or cannot be determined experimentally. In order to estimate these parameters mathematically, we searched for data tracking the biomass changes of *B. thetaiotaomicron*, *E. rectale*, and *M. smithii* in order fit our model to this data with the goal of estimating these parameters. This system, however, does not account for all possible parameters that could potentially affect the fluctuations in biomass or substrate concentration.

From the literature, we were able to obtain longitudinal data on an experiment involving *B. thetaiotaomicron* and its substrates, presented in Adamberg et al. 2014<sup>15</sup>. However, similar longitudinal data on all three species *B. thetaiotaomicron*, *E. rectale*, and *M. smithii* is, to our knowledge, not openly available in the published literature. We were able to extract a single set of data points for the full system including all three species and their relevant substrates from Shoaie et al<sup>11</sup>.

Due to limitations in availability of data for our 3-species model for *B. thetaiotaomicron*, *M. smithii*, and *E. rectale*, we are not able to estimate the remaining model parameters to the same degree of confidence as we were with a reduced system (Appendix B). In our literature review, however, we were able to obtain a single set of endpoint data values for an experiment found in Shoaie et al.<sup>11</sup> conducted on all three species. Given the lack of available longitudinal data for this biological system, we assume that this data, shown in Table 3, are the center values of the oscillations for each substrate or biomass quantity. One complication that arises from using this data is that the total biomass for all three species was experimentally measured as a single quantity, which is another factor that further contributes to our uncertainty in our full model parameter estimates. We fit the model parameters to produce numerical solutions with average biomass concentrations that roughly sum to the biomass quantity given in Table 3. The parameter estimates obtained in Appendix B on a reduced model, including some manual adjustments, allowed us to obtain rough estimates of the remaining parameters in our full model.

Polysaccharides ( $\mu\text{M}$ )	32.06
H <sub>2</sub> ( $\mu\text{M}$ )	0
CO <sub>2</sub> ( $\mu\text{M}$ )	7.96
Acetate ( $\mu\text{M}$ )	9.71
Biomass (gDW)	0.001412

**Table 3.** Table of experimental data presented in Shoaie et al. 2013<sup>11</sup> of the microorganisms *B. thetaiotaomicron*, *E. rectale*, and *M. smithii* and their substrates CO<sub>2</sub>, H<sub>2</sub>, acetate, and polysaccharides. The biomass measurement is a combination of the biomass of the three microorganisms.

	0 hrs	24 hrs	72 hrs
Polysaccharides (mM)	16.12	11.93	2.95
H <sub>2</sub> (mL)	0	0.0045	0.0051
CO <sub>2</sub> (mL)	0	0.0588	0.154
Acetate (mM)	0	3.296	7.46
Biomass (gDW)	$2.34 \times 10^{-5}$	$1.306 \times 10^{-4}$	$2.897 \times 10^{-4}$

**Table 4.** Table for experimental results with data for polysaccharides, H<sub>2</sub>, CO<sub>2</sub>, acetate, and the biomass of *B. thetaiotaomicron* in a medium initially containing with 20 amino acids across distinct time points. Only the bacterial species *B. thetaiotaomicron* was present in the medium. The data contained in this table is originally from Adamberg et al. 2014<sup>15</sup>.

Through fitting the model parameters to the data shown in Table 3, we obtained rough estimates of our model's parameters, which are shown in Table 5. We treated the parameter estimates obtained from the reduced model as initial parameter values

that could be adjusted as needed, rather than a fixed quantity. This choice was made because the experiments conducted to produce the data given in Tables 3 and 4 were performed under different experimental conditions, such as the temperature of environment and the medium the culture grew in, which are factors that could potentially impact the estimates of these parameters.

For the remaining parameters in the model, we assigned values that were of the same magnitude as similar parameters that we estimated in the reduced model. After assessing the fit of the numerical solutions to the data using our initial set of parameter estimates, these estimates were iteratively adjusted in order to reduce the error between the center value of the numerical solution's oscillations and the data value given in Table 3. The resulting parameter estimates based on implementing this approach are given in Table 5.

$\beta_a$	$1.0 \times 10^7$	$\beta_{h_2}$	33,000	$\gamma_B$	10	$\mu_{hM}$	40
$\beta_B$	1.2	$\beta_{M_1}$	0.8	$\gamma_h$	150	$\mu_{pB}$	200,000
$\beta_{E_1}$	0.8	$\beta_{M_2}$	0.5	$\gamma_p$	400	$\mu_{pE}$	5,000
$\beta_{E_2}$	0.6	$\beta_p$	10,000	$\mu_{aE}$	25,000	$q$	0.05
$\beta_{h_1}$	150	$\gamma_a$	200	$\mu_{aM}$	50,000		

**Table 5.** Table of fitted parameter values for equations (1) and (2) based on the experimental data in Table 4.

### Sensitivity Analysis Methods

We utilized global sensitivity analysis in order to identify the driving parameters of our model. In this framework, which utilizes Monte-Carlo (MC) methods, each parameter is assigned a probability density function (pdf) based on *a priori* information known about the parameter. Samples are drawn from the probability density functions (pdfs) to evaluate the overall model output.

Because we are interested in detecting significant nonlinear interactions among the model parameters, implementations of global sensitivity analysis methods for linear relationships like the partial rank correlation coefficient (PRCC), the Pearson correlation coefficient (CC), and standardized regression coefficients (SRC) would not be useful in our case. Consequently, we employed the Sobol' method, a variance-based decomposition method<sup>26</sup>.

Sobol' indices are a MC variance-based approach to calculating all first-order and total-effects indices in a model with  $k$  parameters. These sensitivity indices are computed based on model evaluations for  $N$  simulations. In order to improve the sensitivity estimates, the values tested for each parameter in the model are drawn from quasi-random number generators. Though the use of quasi-random numbers from a given distribution is not necessary, we incorporate this approach into our computations.

We wrote a function in Julia v1.1.1 that computes the first-order and total-order Sobol' indices for a given ODE-based model for each parameter-variable combination, which is included in Appendix A.

To compute the first- and total-order Sobol' indices for our reduced model parameters, we specified prior distributions for each parameter from which to draw samples. Parameter samples are initially drawn from a quasi-random number generator on the interval  $[0, 1]$ . Using the inverse transform sampling method, these samples are transformed into a simulated parameter value based on its specified prior distribution for the sensitivity calculation of the Sobol' indices<sup>27</sup>.

To specify distributions for each parameter in the full model, we first set all but one parameter to a Gamma( $k, \theta$ ) distribution since we expect all of these parameters to be strictly positive. The parameter  $q$  was specified to follow a Beta(5, 95) distribution. Though the support of this distribution restricts the samples to the interval  $[0, 1]$ , we deemed this option to be more appropriate due to the Gamma(0.025, 2.0) distribution's heavy right-skewness and tendency to sample infinitesimally small, unlikely values.

We implemented a similar approach in specifying each  $k$  and  $\theta$  as in the reduced model; the mean of each parameter's distribution was set to be equal to our estimated value in Table 5. The variance was specified to be equal to two times the estimated parameter value. We chose this value for the variance in order to cover a wide range of sample values for our sensitivity analysis due to a large uncertainty in our parameter estimates. Table 1 shows the values of  $k$ ,  $\theta$ , and the mean and variance of each parameter distribution.

### Data availability

The data generated in this modeling and simulation effort is included in the appendices of this manuscript, as well as the Julia code used to generate that data.

	$B$	$E$	$M$	$a$	$h$	$p$
$\beta_a$	0.00	0.00	0.00	0.00	0.00	0.00
$\beta_B$	0.98	0.02	0.01	0.02	0.37	0.13
$\beta_{E_1}$	0.00	0.00	0.00	0.04	0.00	0.00
$\beta_{E_2}$	0.00	0.82	0.01	0.02	0.10	0.03
$\beta_{h_1}$	0.00	0.00	0.00	0.00	0.00	0.00
$\beta_{h_2}$	0.00	0.00	0.00	0.00	0.00	0.00
$\beta_{M_1}$	0.00	0.00	0.04	0.04	0.06	0.00
$\beta_{M_2}$	0.00	0.00	0.65	0.02	0.17	0.00
$\beta_p$	0.00	0.00	0.00	0.00	0.00	0.00
$\gamma_a$	0.00	0.00	0.00	0.00	0.00	0.00
$\gamma_B$	0.00	0.00	0.00	0.00	0.00	0.00
$\gamma_h$	0.00	0.00	0.00	0.00	0.00	0.00
$\gamma_p$	0.00	0.00	0.00	0.00	0.01	0.00
$\mu_{aE}$	0.00	0.00	0.00	0.00	0.00	0.00
$\mu_{aM}$	0.00	0.00	0.00	0.00	0.00	0.00
$\mu_{hM}$	0.00	0.00	0.00	0.00	0.00	0.00
$\mu_{pB}$	0.00	0.00	0.00	0.00	0.00	0.00
$\mu_{pE}$	0.00	0.00	0.00	0.00	0.00	0.00
$q$	0.00	0.01	0.02	0.07	0.02	0.09
Total	0.99	0.85	0.74	0.23	0.75	0.24

**Table 6.** Table of model parameters' estimated first-order Sobol' indices for each output,  $B$ ,  $E$ ,  $M$ ,  $a$ ,  $h$ , and  $p$ , using  $N = 2^{18}$  simulations.

	$B$	$E$	$M$	$a$	$h$	$p$
$\beta_a$	0.00	0.00	0.00	0.00	0.00	0.00
$\beta_B$	0.99	0.13	0.11	0.33	0.56	0.80
$\beta_{E_1}$	0.00	0.01	0.00	0.56	0.01	0.04
$\beta_{E_2}$	0.01	0.97	0.04	0.22	0.18	0.49
$\beta_{h_1}$	0.00	0.00	0.00	0.00	0.00	0.00
$\beta_{h_2}$	0.00	0.00	0.00	0.00	0.00	0.00
$\beta_{M_1}$	0.00	0.00	0.05	0.58	0.10	0.01
$\beta_{M_2}$	0.00	0.00	0.88	0.19	0.25	0.00
$\beta_p$	0.00	0.00	0.00	0.00	0.00	0.00
$\gamma_a$	0.00	0.00	0.00	0.00	0.00	0.00
$\gamma_B$	0.00	0.00	0.00	0.00	0.00	0.00
$\gamma_h$	0.00	0.00	0.01	0.00	0.00	0.00
$\gamma_p$	0.01	0.01	0.00	0.00	0.01	0.00
$\mu_{aE}$	0.00	0.00	0.00	0.00	0.00	0.00
$\mu_{aM}$	0.00	0.00	0.00	0.00	0.00	0.00
$\mu_{hM}$	0.00	0.00	0.04	0.01	0.00	0.00
$\mu_{pB}$	0.00	0.00	0.00	0.00	0.00	0.00
$\mu_{pE}$	0.00	0.00	0.00	0.00	0.00	0.00
$q$	0.01	0.05	0.11	0.62	0.17	0.72
Total	1.02	1.17	1.25	2.48	1.29	2.09

**Table 7.** Table of model parameters' estimated total-order Sobol' indices for each output,  $B$ ,  $E$ ,  $M$ ,  $a$ ,  $h$ , and  $p$ , using  $N = 2^{18}$  simulations.

## References

1. David, L. A. *et al.* Diet rapidly and reproducibly alters the human gut microbiome. *Nature* **505**, 559–563, DOI: [10.1038/nature12820](https://doi.org/10.1038/nature12820).Diet (2014).
2. Ji, B. & Nielsen, J. From next-generation sequencing to systematic modeling of the gut microbiome. *Front. Genet.* **6**, 1–9, DOI: [10.3389/fgene.2015.00219](https://doi.org/10.3389/fgene.2015.00219) (2015).
3. Mangalam, A. K., Yadav, M. & Yadav, R. The emerging world of microbiome in autoimmune disorders: Opportunities and challenges. *Indian journal rheumatology* **16**, 57–72, DOI: [10.4103/injr.injr\\_210\\_20](https://doi.org/10.4103/injr.injr_210_20) (2021).
4. Freedman, S. N., Shahi, S. K. & Mangalam, A. K. The “gut feeling”: Breaking down the role of gut microbiome in multiple sclerosis. *Neurotherapeutics* **1**, 109–125, DOI: [10.1007/s13311-017-0588-x](https://doi.org/10.1007/s13311-017-0588-x) (2018).
5. Cryan, J. F., O’Riordan, K. J., Sandhu, K., Peterson, V. & Dinan, T. G. The gut microbiome in neurological disorders. *Lancet Neurol.* **2**, 179–194, DOI: [10.1016/S1474-4422\(19\)30356-4](https://doi.org/10.1016/S1474-4422(19)30356-4) (2020).
6. Singh, R. K. *et al.* Influence of diet on the gut microbiome and implications for human health. *J Transl Med.* **1**, 73, DOI: [10.1186/s12967-017-1175-y](https://doi.org/10.1186/s12967-017-1175-y) (2017).
7. Cady, N., Peterson, S. R., Freedman, S. N. & Mangalam, A. K. Beyond metabolism: The complex interplay between dietary phytoestrogens, gut bacteria, and cells of nervous and immune systems. *Front. Neurol.* **11**, 150, DOI: [10.3389/fneur.2020.00150](https://doi.org/10.3389/fneur.2020.00150) (2020).
8. Kumar, M., Ji, B., Zengler, K. & Nielsen, J. Modelling approaches for studying the microbiome. *Nat. Microbiol.* **4**, 1253–1267, DOI: [10.1038/s41564-019-0491-9](https://doi.org/10.1038/s41564-019-0491-9) (2019).
9. Oreskes, N., Shrader-Frechette, K. & Belitz, K. Verification, validation, and confirmation of numerical models in the earth sciences. *Science* **263**, 641–646, DOI: [10.1126/science.263.5147.641](https://doi.org/10.1126/science.263.5147.641) (1994).
10. Smith, H. L. & Waltman, P. *The Theory of The Chemostat: Dynamics of Microbial Competition* (Cambridge University Press, 2008).
11. Shoaie, S. *et al.* Understanding the interactions between bacteria in the human gut through metabolic modeling. *Sci. Reports* **3**, 1–10, DOI: [10.1038/srep02532](https://doi.org/10.1038/srep02532) (2013).
12. Kim, M. H. & Kim, H. The roles of glutamine in the intestine and its implication in intestinal diseases. *Int. J. Mol. Sci.* **18**, DOI: [10.3390/ijms18051051](https://doi.org/10.3390/ijms18051051) (2017).
13. Scaldaferrri, F. *et al.* Intestinal gas production and gastrointestinal symptoms: from pathogenesis to clinical implication. *Eur. review for medical pharmacological sciences* **17**, 2–10 (2013).
14. Xu, J. *et al.* A genomic view of the human-Bacteroides thetaiotaomicron symbiosis. *Science* **299**, 2074–2076, DOI: [10.1126/science.1101000](https://doi.org/10.1126/science.1101000) (2003).
15. Adamberg, S. *et al.* Degradation of fructans and production of propionic acid by Bacteroides thetaiotaomicron are enhanced by the shortage of amino acids. *Front. Nutr.* **1**, 1–10, DOI: [10.3389/fnut.2014.00021](https://doi.org/10.3389/fnut.2014.00021) (2014).
16. Martens, E. C. *et al.* Recognition and degradation of plant cell wall polysaccharides by two human gut symbionts. *PLoS Biol.* **9**, DOI: [10.1371/journal.pbio.1001221](https://doi.org/10.1371/journal.pbio.1001221) (2011).
17. Glass, T. L. & Hylemon, P. B. Characterization of a pyridine nucleotide-nonspecific glutamate dehydrogenase from bacteroides thetaiotaomicron. *J. Bacteriol.* **141**, 1320–1330 (1980).
18. Mahowald, M. A. *et al.* Characterizing a model human gut microbiota composed of members of its two dominant bacterial phyla. *Proc. Natl. Acad. Sci. United States Am.* **106**, 5859–5864 (2009).
19. Saltelli, A. *et al.* *Global Sensitivity Analysis. The Primer*, chap. 1-6, i–xi (John Wiley & Sons, Ltd, 2008). <https://onlinelibrary.wiley.com/doi/pdf/10.1002/9780470725184.fmatter>.
20. Iooss, B. & Prieur, C. Shapley effects for sensitivity analysis with correlated inputs: Comparisons with sobol’ indices, numerical estimation and applications. *Int. J. for Uncertain. Quantification* **9**, 493–514, DOI: [10.1615/Int.J.UncertaintyQuantification.2019028372](https://doi.org/10.1615/Int.J.UncertaintyQuantification.2019028372) (2019). [1707.01334](https://doi.org/10.1615/Int.J.UncertaintyQuantification.2019028372).
21. Rabitz, H. Sixth International Conference on Sensitivity Analysis of Model Output Global Sensitivity Analysis for Systems with Independent and / or Correlated Inputs. *Soins Aides-soignantes* **2**, 7587–7589, DOI: [10.1016/j.sbspro.2010.05.131](https://doi.org/10.1016/j.sbspro.2010.05.131) (2010).
22. Jangi, S. *et al.* Alterations of the human gut microbiome in multiple sclerosis. *Nat. Commun.* **7**, DOI: [10.1038/ncomms12015](https://doi.org/10.1038/ncomms12015) (2016).

23. Monod, J. The growth of bacterial cultures. *Ann. Rev. Microbiol.* **3**, 371–394 (1949).
24. Stefan, M. I. & Le Novère, N. Cooperative Binding. *PLoS Comput. Biol.* **9**, e1003106, DOI: [10.1371/journal.pcbi.1003106](https://doi.org/10.1371/journal.pcbi.1003106) (2013).
25. Voit, E. O. *Computational Analysis of Biochemical Systems: A Practical Guide for Biochemists and Molecular Biologists* (Cambridge University Press, 2000).
26. Marino, S., Hogue, I. B., Ray, C. J. & Kirschner, D. E. A methodology for performing global uncertainty and sensitivity analysis in systems biology. *Microbiology* **254**, 178–196, DOI: [10.1016/j.jtbi.2008.04.011](https://doi.org/10.1016/j.jtbi.2008.04.011).A (2009).
27. Devroye, L. General principles in random variate generation. In *Non-Uniform Random Variate Generation*, chap. 2, 27–82 (Springer, 1986).

## Author contributions statement

M.A. translated the biological system to a schematic, wrote the Julia code, and conducted the numerical simulations and sensitivity analyses. M.A. and B.A. created the mathematical models. M.A. and A.M. related the models and underlying biology to each other. B.A. conceived of the project. All authors contributed to the writing of the manuscript and reviewed the manuscript.

## Additional information

### Competing interests

The authors declare no competing interests.

## A Appendix A: Julia Code for First- and Total-Order Sobol' Indices

```

"""
sobol(f, N, u0, tspan, t, k, θ, index = "first-order")

Creates a matrix of Sobol' sensitivities where each row contains
the sensitivity indices for a parameter across different model
outputs.

f - system of ODEs
N - number of simulations (can vary from hundreds to thousands)
u0 - vector of initial conditions for ODE
tspan - time span
k - vector of scale parameters from Gamma(ki, θi) for all
    model parameters
θ - vector of shape parameters from Gamma(ki, θi) for all
    model parameters
index - default is the first order index, but can take on the
        other value "total-order"
t - specified time in tspan to evaluate each model variable
"""

using Sobol
using Distributions
function sobol(f, N, u0, tspan, k, θ, index = "first-order",
              t = 5)
    K = length(k)
    vars = length(u0)
    # quasi-randomly selected points
    S = zeros(N, 2*K)
    s = SobolSeq(2*K)
    θ = [θ; θ]
    k = [k; k]

```

```

S = zeros(N,2*K)
for sim in 1:N
    S[sim,:] = next!(s)

    for parameter in 1:2*K
        S[sim,parameter] = quantile(Gamma(k[parameter],
            θ[parameter]), S[sim,parameter])
    end
end

A = S[:, 1:K] # accounts for half of the random sample
B = S[:, (K+1):2*K] # accounts for second half of the
                    # random sample

sums = zeros(4,vars)
ya = solveODE(f, u0, vars, tspan, t, A, N)
yb = solveODE(f, u0, vars, tspan, t, B, N)
sumC = zeros(K,vars) # (parameter, variable)

for p in 1:K # iterates through changing one column of C at
             # a time (parameters)
    C = Ci(p,A,B)
    yc = solveODE(f, u0, vars, tspan, t, C, N)

    for v in 1:vars
        if index == "first-order"
            sumC[p,v] = yc[:,v]'*ya[:,v]/N

        else
            sumC[p,v] = yc[:,v]'*yb[:,v]/N
        end
    end
end

sens = zeros(K,vars) # (parameter, variable)

for v in 1:vars
    sums[1,v] = ya[:,v]'*ya[:,v]/N

                # sum(ya^2)/N

    sums[2,v] = (sum(ya[:,v])/N)^2 # [sum(ya)/N]^2
    sums[3,v] = sums[1,v] - sums[2,v]
                # denominator for sensitivity calculation
    sums[4,v] = sum(yb[:,v])*sum(ya[:,v])/N.^2
                # sum(ya)*sum(yb)/N^2

    for p in 1:K
        if index == "first-order"
            sens[p,v] = (sumC[p,v] - sums[4,v])/sums[3,v]
        else
            sens[p,v] = 1 - (sumC[p,v] - sums[2,v])/sums[3,v]
        end
    end
end

```

```

        end
    end
    return sens # matrix of sensitivity indices
end

"""
Ci(i, A, B)

Creates a new matrix C by replacing the ith column of matrix B
with the ith column of matrix A.

i - column number to be changed in matrix B
A - matrix containing half of the pseudo-random samples
B - matrix containing the other half of the pseudo-random
    samples
"""

function Ci(i, A, B)
    C = zeros(size(B))
    for j in 1:size(A)[2]
        if j == i
            C[:,i] = A[:,i]
        else
            C[:,j] = B[:,j]
        end
    end
    return C
end

"""
solveODE(f, u0, vars, tspan, t, M, N)

Solves the system of ODEs f and creates a matrix of model
evaluations for each simulation and output variable. Each row
corresponds to model solutions at a given time t for one
simulation.

f - system of ODEs
u0 - vector of initial conditions for the ODEs
vars - number of output variables
tspan - time span
t - specified time in tspan to evaluate each model variable
M - matrix with rows as parameter values and columns as
    simulations
N - number of simulations (can vary from hundreds to thousands)
"""

function solveODE(f, u0, vars, tspan, t, M, N)
    y = zeros(N, vars) # (simulation, variable)
    for sim in 1:N
        p = M[sim, :]
        prob = ODEProblem(f, u0, tspan, p)
        sol = solve(prob)
        for variable in 1:vars
            y[sim, variable] = sol.u[t][variable]
        end
    end
end

```

```

end
return y # matrix of model outputs
end

```

## B Appendix B: Reduced System

Table 1 presents data found in Adamberg et al. 2014<sup>15</sup>. The experiment conducted in this paper focused on *B. thetaiotaomicron* with the substrates H<sub>2</sub>, CO<sub>2</sub>, acetate, and polysaccharides. We utilized this data for parameter determination and estimation by condensing our model to only include *B. thetaiotaomicron* and its substrates.

	0 hrs	24 hrs	72 hrs
Polysaccharides (mM)	16.12	11.93	2.95
H <sub>2</sub> (mL)	0	0.0045	0.0051
CO <sub>2</sub> (mL)	0	0.0588	0.154
Acetate (mM)	0	3.296	7.46
Biomass (gDW)	$2.34 \times 10^{-5}$	$1.306 \times 10^{-4}$	$2.897 \times 10^{-4}$

**Table 8.** Table for experimental results with data for polysaccharides, H<sub>2</sub>, CO<sub>2</sub>, acetate, and the biomass of *B. thetaiotaomicron* in a medium initially containing with 20 amino acids across distinct time points. Only the bacterial species *B. thetaiotaomicron* was present in the medium. The data contained in this table is originally from Adamberg et al. 2014<sup>15</sup>.

The subsystem isolating *B. thetaiotaomicron*'s metabolism is illustrated in Figure 6. Based on this graphical representation, we extracted the reduced system from our full model in equations (1) and (2), producing the reduced system of ODEs in equations (5). Terms related to chemostatic flow were removed because the experimental data in Table 8 was collected in a closed system, rather than an open system like a chemostat. Lastly, we removed any terms that account for an input of polysaccharides because only a specified initial amount was placed in the experimental device for *B. thetaiotaomicron* to consume over time.



**Figure 6.** Graphical representation of a subset of *B. thetaiotaomicron*'s metabolism, including the utilization of polysaccharides and the production of acetate, CO<sub>2</sub>, and H<sub>2</sub>. This diagram is based on information presented in Adamberg et al. 2014<sup>15</sup>.

$$\frac{dB}{dt} = \beta_B \Psi_{\gamma_p}(p)B \quad (5a)$$

$$\frac{da}{dt} = \beta_a \Psi_{\gamma_p}(p)B \quad (5b)$$

$$\frac{dh}{dt} = \beta_{h_2} \Psi_{\gamma_p}(p)B \quad (5c)$$

$$\frac{dp}{dt} = -\mu_{p,B}Bp \quad (5d)$$

By fitting our reduced model to the collected data in Table 8, we estimated the model parameters using the Julia packages `DiffEqParamEstim` and `Optim` with the goal of utilizing these results to inform our full model parameter estimation. We ultimately chose the simulated annealing method to apply to our optimization problem.

In the first step of finding a roughly optimal solution for our reduced model's parameters, we first chose an arbitrary vector of initial values for these parameters. Once we chose these arbitrary initial values, we used the `DiffEqParamEstim` and `Optim` packages in order to obtain the optimal results given by the simulated annealing method. The results produced from this constrained optimization given our initial guess of parameter values allowed us to achieve a seemingly local optimum for the system. We utilized this output by adjusting the output parameter values ourselves in order to further reduce the residuals. Using this new set of parameters, we reran the optimization once more in the hopes of producing a better fit to the data.

Figures 7, 8, and 9 show the solutions to our system of ODEs using our final set of roughly optimized parameters in Table 9 based on the data in Table 8.

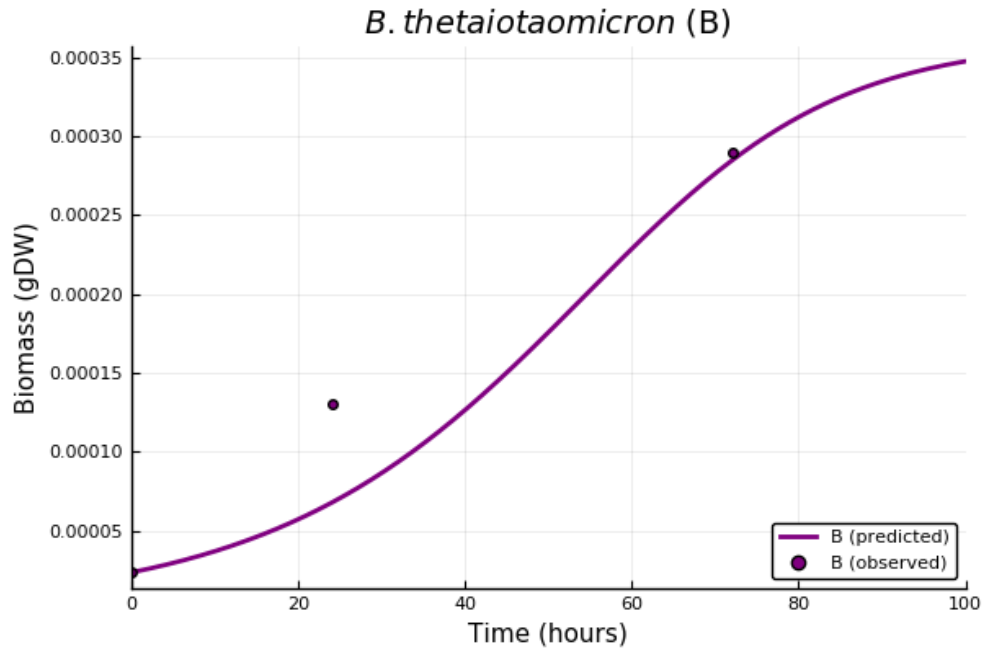


**Figure 7.** Plot of the solutions to equation (5a) and the observed data for *B. thetaiotaomicron* over the time interval 0 to 72 hours.

$\beta_a$	$\beta_B$	$\beta_{h_2}$	$\gamma_p$	$\mu_{pB}$
2000	0.08	50	10	200

**Table 9.** Table of fitted parameter values for equations (5) based on the experimental data in Table 8.

#### **First- and Total-Order Sobol' Indices for the Reduced Model Parameters**

In order to specify the distribution of our model's parameters, we first considered the domain of each parameter. All parameters in our reduced model can reasonably take on positive values, so we restricted our consideration to parameter distributions defined on the positive number line. Due to its positive, continuous domain, we chose the Gamma( $k, \theta$ ) distribution as the general form of our specified parameter distributions. Using the results of our parameter estimation in Table 9, we defined the mean of the Gamma distributions to be equal to the estimates we obtained from our parameter estimation. Because we obtained one set of parameter estimates for our reduced model, we are not able to obtain an informed variance on our parameter distributions. In order to reflect our minimal knowledge of the true parameter values, we define the variance of these Gamma distributions to be large in order to test a wide range of parameter values in our sensitivity calculations, which are specified in Table 10.

The first- and total-order results of the sensitivity analysis of the parameters in our reduced model are presented in Tables 11 and 12. Based on the small changes observed from the first-order sensitivities compared to the total-order sensitivities, we can conclude that higher order parameter interactions do not significantly contribute to the variance of the model outputs, so these higher order interactions can safely be ignored. From the sensitivity results, it can be concluded that the parameter  $\beta_B$  is influential on the variance of the model outputs due to  $\beta_B$ 's high sensitivity indices for all outputs. An unexpected result

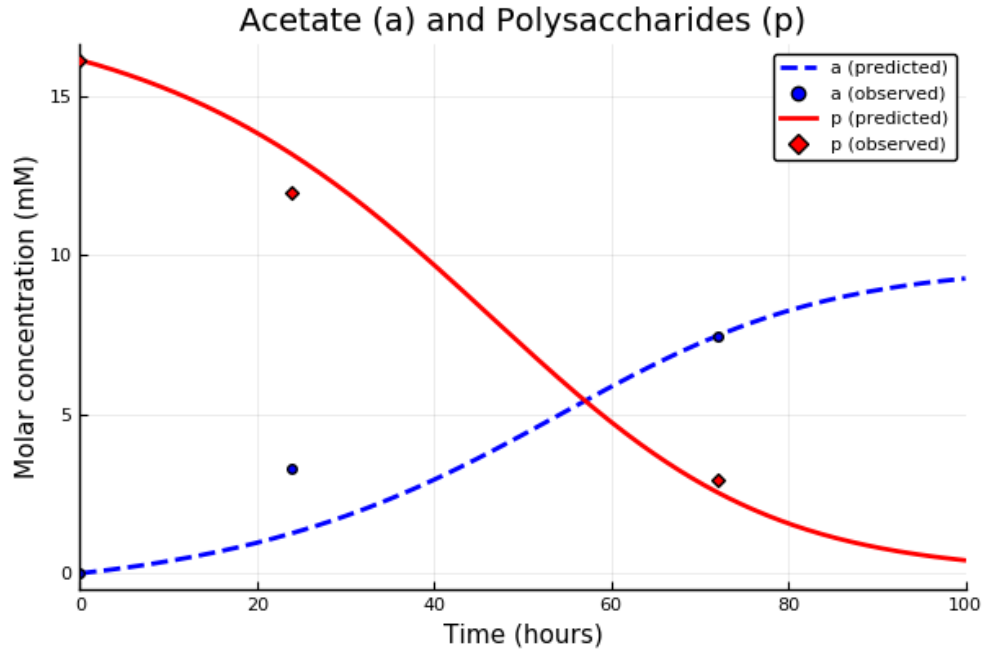


**Figure 8.** Plot of the solutions to equations (5b) and (5d), as well as the observed data for acetate and polysaccharides over the time interval 0 to 72 hours.

	$k$	$\theta$	Mean	Variance
$\beta_a$	2000	1	2000	2000
$\beta_B$	0.01	8	0.08	0.64
$\beta_h$	50	1	50	50
$\gamma_p$	10	1	10	10
$\mu_{pB}$	200	1	200	200

**Table 10.** Table of defined parameter distributions for the parameters in our reduced model, including the mean and variance of the distribution.

based on these indices is that the variable  $p$  is more sensitive to changes in the parameter  $\gamma_p$ , the Michaelis-Menten constant in the Monod form, than  $\mu_{pB}$ , the rate *B. thetaiotaomicron* consumes polysaccharides. Though  $\gamma_p$  explains more variance in  $p$  than  $\mu_{pB}$ , the first- and total-order effects for this parameter are relatively low compared to the main effects of parameter  $\beta_B$ , which appears to be the driving parameter of this subsystem. Overall, the results obtained in Tables 11 and 12 are generally unsurprising and intuitive. With these parameter estimates and Sobol' indices in mind, we then utilized this information in our full model to conduct a sensitivity analysis of all nineteen parameters.

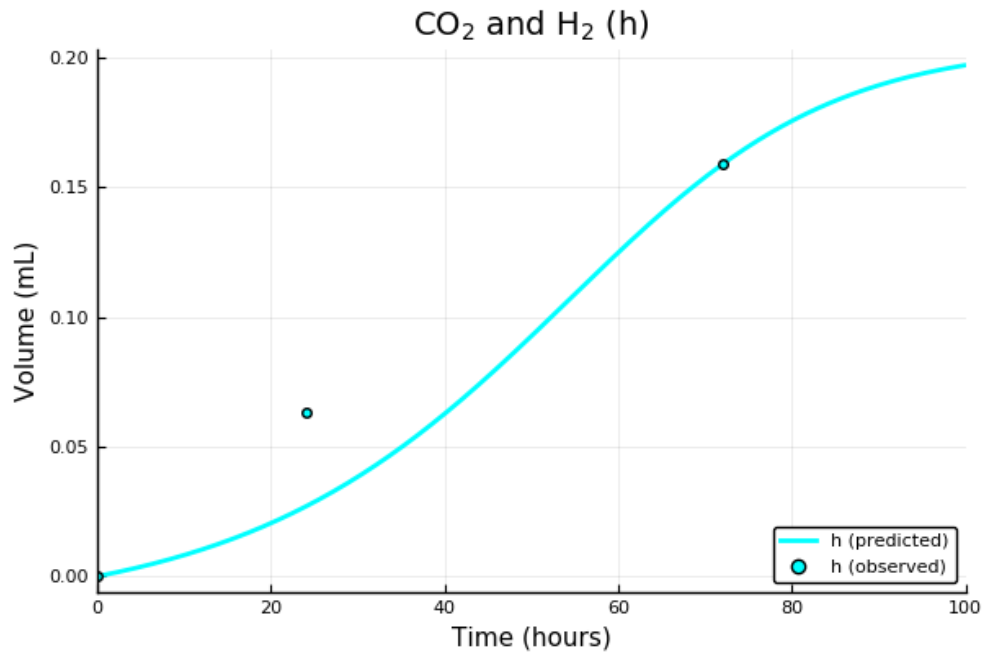


**Figure 9.** Plot of the solutions to equation (5c) and the observed data for CO<sub>2</sub> and H<sub>2</sub> over the time interval 0 to 72 hours.

	$B$	$a$	$h$	$p$
$\beta_a$	0.000	0.003	0.002	0.003
$\beta_B$	0.995	0.838	0.572	0.891
$\beta_h$	0.000	0.000	0.304	0.000
$\gamma_p$	0.000	0.120	0.080	0.064
$\mu_{pB}$	0.000	0.025	0.017	0.034
Total	0.995	0.982	0.974	0.992

**Table 11.** Table of first-order Sobol' indices for our reduced model in equations (5) using  $N = 2^{18}$  simulations.

	$B$	$a$	$h$	$p$
$\beta_a$	0.003	0.003	0.002	0.002
$\beta_B$	1.000	0.856	0.596	0.898
$\beta_h$	0.002	0.001	0.318	0.000
$\gamma_p$	0.003	0.133	0.092	0.072
$\mu_{pB}$	0.002	0.030	0.021	0.035
Total	1.010	1.012	1.028	1.007

**Table 12.** Table of total-order Sobol' indices for our reduced model in equations (5) using  $N = 2^{18}$  simulations.